This article has been accepted for publication in a future issue of this journal, but has not been fully edited. Content may change prior to final publication. Citation information: DOI 10.1109/TSUSC.2019.2896667, IEEE Transactions on Sustainable Computing

Censor-Based Cooperative Multi-Antenna Spectrum Sensing with Imperfect Reporting Channels

Meiling Li, *Member, IEEE*, Omar Alhussein, *Student Member, IEEE*, Paschalis C. Sofotasios, *Senior Member, IEEE*, Sami Muhaidat, *Senior Member, IEEE*, Paul D. Yoo, *Senior Member, IEEE*, Jie Liang, *Senior Member, IEEE*, and Anhong Wang

Abstract—The present contribution proposes a spectrally efficient censor-based cooperative spectrum sensing (C-CSS) approach in a sustainable cognitive radio network that consists of multiple antenna nodes and experiences imperfect sensing and reporting channels. In this context, exact analytic expressions are first derived for the corresponding probability of detection, probability of false alarm and secondary throughput, assuming that each secondary user (SU) sends its detection outcome to a fusion center only when it has detected a primary signal. Capitalizing on the findings of the analysis, the effects of critical measures, such as the detection threshold, the number of SUs and the number of employed antennas, on the overall system performance are also quantified. In addition, the optimal detection threshold for each antenna based on the Neyman-Pearson criterion is derived and useful insights are developed on how to maximize the system throughput with a reduced number of SUs. It is shown that the C-CSS approach provides two distinct benefits compared with the conventional sensing approach, i.e., without censoring: i) the sensing tail problem, which exists in imperfect sensing environments, can be mitigated; ii) less SUs are ultimately required to obtain higher secondary throughput, rendering the system more sustainable.

Index Terms—Sustainble computing, energy efficiency, energy detection, cooperative spectrum sensing, censoring, imperfect reporting channels, multi-antenna systems.

1 Introduction

M. Li and A. Wang are with the School of Electronics Information Engineering, Taiyuan University of Science and Technology, 030024 Taiyuan, China (email: meiling_li@126.com; wah_ty@163.com*)*
O. Alhussein was with the School of Engineering Science, Simon Fraser University, Burnaby, BC V5A 1S6, Canada. He is now with the Department of Electrical and Computer Engineering, University of Waterloo, ON N2L 3G1, Waterloo, Canada (e-mail: oalhusse@uwaterloo.ca*)*
P. C. Sofotasios is with the Center for Cyber-Physical Systems, Department of Electrical and Computer Engineering, Khalifa University, PO Box 127788, Abu Dhabi, UAE and with the Department of Electronics and Communications Engineering, Tampere University of Technology, 33101, Tampere, Finland (e-mail: p.sofotasios@ieee.org*)*
S. Muhaidat is with the Center for Cyber-Physical Systems, Department of Electrical and Computer Engineering, Khalifa University, PO Box 127788, Abu Dhabi, UAE and with the Department of Electronic Engineering, University of Surrey, GU2 7XH, Guildford, UK (e-mail: muhaidat@ieee.org*)*
P. D. Yoo is with Department of Computer Science and Information Systems, Birkbeck College, University of London, WC1E 7HX, London, UK (e-mail: paul.d.yoo@ieee.org*)*
J. Liang is with the School of Engineering Science, Simon Fraser University, BC V5A 1S6, Burnaby, Canada (e-mail: jiel@sfu.ca)

COGNITIVE radio networks (CRNs) have been proposed as an effective approach to address the current scarcity in frequency spectrum resources [1]. In light of this, CRNs lead to a significant increase of spectrum utilization due to the spectrum sensing capability of such systems, particularly in collaborative configurations. In general, CR systems consist of at least a primary user (PU), that is typically assigned licensed frequency bands, and a secondary user (SU) that attempts to access the licensed spectrum when underutilized. This is practically realized by means of three different approaches namely, overlay, underlay, and interweave (i.e., opportunistically) [1]. The present contribution is concerned with the third approach, in which a secondary user attempts to access the spectrum when the primary user is idle. Hence, there is a need for a highly accurate and effective spectrum sensing technique that will ensure sufficient interference avoidance to primary user(s).

Several spectrum sensing (SS) techniques that mainly focus on achieving an improved sensing performance and/or a reduction of the overall system complexity have been proposed in the past few years. In this context, energy detection (ED) is widely considered among the most common detection methods and has received considerable attention owing to its relatively low computational and implementation complexity. Nevertheless, the non-cooperative ED-based approach has been shown to be susceptible to the so-called hidden terminal problem. This phenomenon occurs when the SU is subject to non-negligible fading or path-loss effects while the PU is still in operation, thereby hindering an efficient detection of the PU. Thus, cooperative spectrum sensing (CSS) has been proposed as an effective method to improve the sensing performance by exploiting the spatial diversity among multiple SUs.

There are two successive phases in CSS: sensing phase and reporting phase. During the second phase, time division multiple access (TDMA) scheme is often assumed, where multiple SUs report their local sensing results to a fusion center (FC) in different time slot, in

This article has been accepted for publication in a future issue of this journal, but has not been fully edited. Content may change prior to final publication. Citation information: DOI 10.1109/TSUSC.2019.2896667, IEEE Transactions on Sustainable Computing

which the focus is mainly on the optimal sensing time during the first phase. Longer sensing duration results in an improved sensing performance at the expense of increased waiting time for SUs to access the channel which ultimately can lead to lower spectrum utilization. One way to resolve such issue is to allow SUs to send their decisions on orthogonal frequency bands. However, more secondary users require larger bandwidth for the reporting channels, which requires effective optimization of the resource consumption of systems, while guaranteeing an acceptable sensing detection performance [2], [3]. Majority of CSS schemes in the open literature rely on on a conventional decision collection approach, in which SUs report all their decisions to the FC with the assumption of TDMA scheme in the reporting phase. Hereafter, we will refer to this approach as traditional (non-censor-based) CSS (T-CSS).

More recently, censor-based CSS (C-CSS) was proposed as an effective method that can reduce the incurred signaling costs in the decisions, which are detrimental in spectrum sensing. In C-CSS, the collaborative SUs report their decisions based on certain conditions rather than periodically [4]–[7].

In contrast to T-CSS literature, there are important issues related to C-CSS schemes that have not been investigated in the open technical literature. How to reduce the cooperation overhead and the system resource consumption while guaranteeing good sensing performance is yet one of the crucial issues in CSS. Hence, there should be a tradeoff between sensing efficiency and sensing accuracy. In addition, the hidden terminal problems exist not only in sensing channels but also in reporting channels, while the CSS performance is usually limited by the imperfect reporting channels.

Motivated by this, the present work is devoted to the analysis of multi-antenna based C-CSS under imperfect sensing and reporting channels. The extent of the safe operation of the PU is quantified in relation to the probability of detection, while the corresponding spectrum efficiency is determined in relation with the respective probability of false alarm. Furthermore, we optimize the secondary throughput through three key influencing metrics, namely the number of the secondary users, the number of the antennas, and the detection threshold. In doing so, we show the theoritical improvements of the C-CSS over the T-CSS, especially under realistic imperfect sensing and reporting channel conditions. Specifically, the contributions of this work are as follows:

- We investigate the relationship among the number of SUs, the number of antennas, the detection threshold, the sensing bandwidth, the spectrum utilization, and the secondary throughput in the considered C-CSS setup. We quantify the performance of both T-CSS and C-CSS under imperfect sensing and reporting channels, and derive simple analytic expressions for the corresponding probability of detection, probability of false alarm and the secondary throughput.

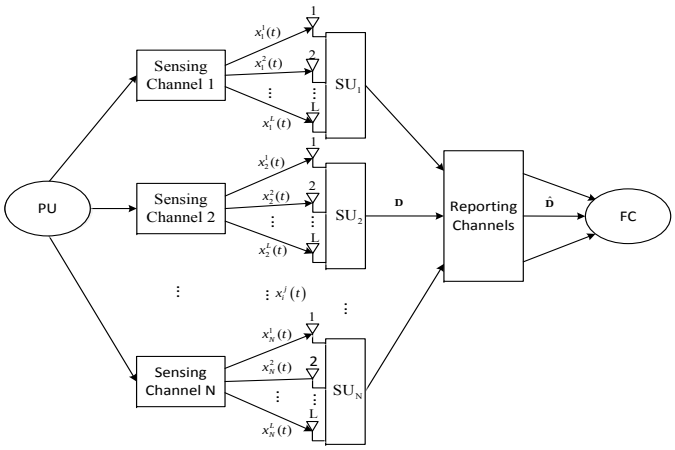

Fig. 1: Multiple antenna sensing network configuration.

- We derive lower bounds for the probability of false alarm, and we show that the sensing tail problem, which exist in the T-CSS, can be mitigated with the aid of C-CSS.
- We analyze the optimal detection threshold that maximizes the secondary throughput when the target probability of detection is satisfied, and propose an optimal algorithm based on the Neyman-Pearson criterion.
- We provide useful insights on how to maximize the secondary throughput in the considered C-CSS scheme.

The remainder of this paper is organized as follows: Section 2 presents an overview of some related works. Section 3 describes the underlying system model for the considered T-CSS and C-CSS. In Section 4, we derive various performance metrics for the non-cooperative and cooperative configurations for both T-CSS and C-CSS schemes with imperfect sensing and reporting channels. In addition, we derive lower bounds for the probability of false-alarm in Section 4.4. Moreover, we demonstrate useful insights on the detection performance trends that are useful in maximizing the secondary throughput. In Section 5, we provide a solution for the problem of optimizing the secondary throughput. Section 6 presents the corresponding numerical results and findings, followed by some closing remarks in Section 7.

2 Related Works

The majority of CSS works rely on the non-censored based approach (T-CSS), in which all decisions collected by secondary users are unconditionally forwarded to the FC. In what follows, we discuss existing T-CSS and C-CSS contributions.

Ganesan and Li [8] considered periodic spectrum sensing and proposed multiple user cooperation methods in the presence of additive white Gaussian noise (AWGN) [9]. The optimal number of users in a CSS scheme over sensing channels in the presence of shadowing and relay

This article has been accepted for publication in a future issue of this journal, but has not been fully edited. Content may change prior to final publication. Citation information: DOI 10.1109/TSUSC.2019.2896667, IEEE Transactions on Sustainable Computing

fading was addressed in [10]–[12]. There, it was also proved that CSS reduces the required average signal-to-noise ratio (SNR) in the sensing phase. Likewise, the authors in [13]–[17] analyzed the crucial relationship between sensing time, secondary throughput, and spectrum utilization. Optimal sensing duration was investigated [18]–[21] in an attempt to improve the overall system throughput, taking into account that a smaller number of SUs leads to a reduced sensing duration at the expense of reduced sensing diversity. Firouzabadi *et al*. [22] considered wideband spectrum sensing and formulated the sensing problem as an optimization problem with the purpose of maximizing the opportunistic throughput of CRN by assuming the number of samples used to report the sensing decisions to the FC, the number of the sensing samples, the detection threshold and the overall sensing-plus-reporting time. Unlike previous work [18]–[22] whose optimization objectives were to maximize the secondary throughput, Zheng *et al*. [23] proposed joint optimization of sensing time and the detection threshold with the aim of maximizing the energy efficiency of cognitive sensor networks.

Liu *et al*. [24] proposed a group-based cooperative medium access control protocol to solve the tradeoff between sensing accuracy and efficiency. Deng *et al*. [25] considered optimal sensor scheduling to realize energy-efficient CSS. Zheng [26] considered OFDM modulation to send each SU's result to the FC. Li [27] proposed a kind of random broadcast scheme in exchanging the sensing results to reduce the signaling cost in reporting phase, while in similar method, Noh [28] proposed controlling the reporting order of the local test statistics to reduce the reporting time. Zhang *et al*. [29] investigated the optimal number of sensing users required to minimize the total error probability, while achieving an adequate tradeoff between the overall detection performance and the control bandwidth used by each SU to report its sensing results. More recently, the authors in [30] investigated the joint effects of radio frequency impairments on the performance of ED-based CSS environment. To this end, novel expressions were derived for the probability of false-alarm and probability of detection in the presence of Rayleigh fading conditions assuming both error-free and imperfect reporting channels.

When considering specific imperfect reporting channel, Lee analyzed the T-CSS performance over Rayleigh reporting channel [31], while several works studied spectrum sensing and T-CSS under generalized or composite fading conditions [32]–[37]. For example, da Costa *et al*. [32] investigated the outage probability performance of a dual-hop decode-and-forward T-CSS scheme under the presence of Nakagami-m fading and interference conditions as well as the effects of fading severity, SU relay placement, the number of PU and SU nodes on the end-to-end T-CSS performance. Likewise, Sofotasios *et al*. [35] investigated the performance of ED-based T-CSS under different diversity receptions in the presence of both generalized and extreme multipath fading conditions, which are typically encountered in enclosed areas such as malls and tunnels. More recently, the performance of T-CSS with multi-antenna nodes over generalized and composite fading channels was analyzed in [36], [37] with the aid of the generic and semi-analytic mixture Gamma (MG) distribution. Moreover, the optimal fusion rule and the number of antennas that minimize the total error rate in the square-law selection (SLS) framework were also analyzed. Yet, accurate optimization of the detection threshold was not addressed in [36], [37]. It is also noted that Li *et al.* [38] proposed interesting tradeoffs in T-CSS, namely: i) the impact of the number of sensing users on spectrum utilization and secondary throughput; and ii) the relationship between the detection threshold, detection performance and secondary throughput.

As mentioned, T-CSS based schemes increase the detection performance and resolve the hidden terminal problem which is present in non-cooperative schemes. However, they incur extra signalling overhead, and can be unnecessarily determental to the detection performance under imperfect sensing and reporting channels. More recently, censor-based CSS (C-CSS) was proposed as an effective method to reduce the signalling costs and improve the network's throughput [39]. In C-CSS, the collaborative SUs report their decisions based on certain conditions. For instance, a censor-based sensor can forward the decision only when it has detected a certain signal. On other instances, it can forward its decision only when the corresponding reporting channel is deemed reliable. Based on this, Rago *et al*. [4] firstly analyzed the performance of censor-based sensors in decentralized detection systems, where only the likelihood ratios of sufficient level of confidence are allowed to transmit to the common receiver over perfect reporting channels. Jiang *et al*. [5] considered a realistic scenario where censor-based detection is performed over imperfect reporting channels assuming that the probability of a present PU is sufficiently low. Likewise, Yiu *et al*. [6] analyzed the ED-based detection performance of a non-orthogonal signaling scheme for the transmission of censored decisions and non-coherent fusion rules. Sun et al. [24] investigated the detection performance of a censoring method with quantization to decrease the average number of transmitted bits, where only reliable information (bits) are considered in the FC over perfect and imperfect reporting channels. In [24], both binary results of 0 (not present) and 1 (present) are transmitted to the FC, where the quantization is subject to optimization. Liu *et al.* [40] proposed a hierarchical cooperative spectrum sensing scheme based on two-threshold energy detection in CRNs, in which soft combination of the observed energy were used to solve the sensing failure problem.

In this paper, we provide a comprehensive study that shows theoretical improvements in using multi-antenna C-CSS scheme under imperfect sensing and reporting channels, when compared to its T-CSS counterpart. That is, we investigate the relationship among the number of

This article has been accepted for publication in a future issue of this journal, but has not been fully edited. Content may change prior to final publication. Citation information: DOI 10.1109/TSUSC.2019.2896667, IEEE Transactions on Sustainable Computing

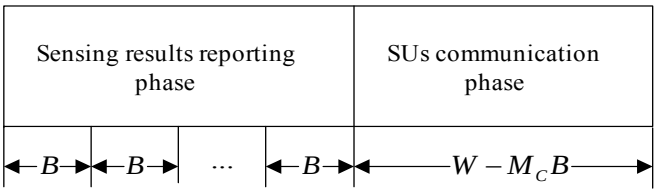

Fig. 2: The bandwidth allocation in C-CSS.

SUs, the number of antennas, the detection threshold, the sensing bandwidth, the spectrum utilization, and the secondary throughput in the considered C-CSS setup. More notably, we derive lower bounds for the probability of false alarm, and we show that the sensing tail problem, which exist in the T-CSS, can be effectively mitigated with the aid of C-CSS. Finally, we analyze optimal detection threshold that maximizes the secondary throughput when the target probability of detection is satisfied, and propose an optimal optimization algorithm based on the Neyman-Pearson criterion.

3 C-CSS System Model

We consider the CSS network configuration in Fig. 1. It consists of one PU and N SU nodes, each of them equipped with L antennas. The considered C-CSS process can be described in the following three steps:

Step 1: We let SU_i^j represent the i^{th} SU node equipped with the j^{th} antenna. Each SU node determines the local decision D_i by combining the results of L antennas, and then deciding on the presence of a PU signal.

Step 2: Each SU node forwards its binary decision to the FC via a reporting channel *only* if the corresponding local decision is equal to unity, i.e. if $D_i = 1$. The set of transmitted decisions are denoted by $\hat{\mathbf{D}} = \{D_1, D_2, \ldots, D_{M_C}\}$, where M_C represents the number of transmitted decisions. Similarly, the transmitted decisions in T-CSS are denoted by $\mathbf{D} = \{D_1, D_2, ..., D_N\}$, where $M_C \leq N$. Furthermore, the local results for all SUs are transmitted to the FC using orthogonal frequency division multiple-access (OFDMA), as illustrated in Fig. 2, where W and B resemble the total bandwidth and the control channel bandwidth used by each SU to report its local decision, respectively.

Step 3: At the FC, all binary decisions are fused together and a final decision is made based on the k-out-of-n rule.

4 Proposed Censor-based Spectrum Sensing

4.1 Non-cooperative Detection

We commence by analyzing the single user performance. To this end, let $x_i^j(t)$ represent the observed signal at the j^{th} antenna of the i^{th} node at time t, and $\mathcal{H}_0$ and $\mathcal{H}_1$ denote the hypotheses for the absence and presence of a PU signal, respectively. Thus, the observed signal can be represented as

$$x_i^j(t) = \begin{cases} n_i^j(t), & \mathcal{H}_0 \\ h_i^j s(t) + n_i^j(t), & \mathcal{H}_1 \end{cases} \tag{1}$$

where $n_i^j(t)$ is $\mathcal{CN}(0, \sigma_n^2)$ denoting the circularly symmetric complex white additive Gaussian noise (AWGN) in the secondary user channel SU_i^j, $s(t)$ is the information signal transmitted by the PU with energy

$$E_s = \mathbb{E}\{|s(t)^2|\} \tag{2}$$

and h_i^j is the complex Gaussian channel gain of the sensing channel between the PU and SU_i^j, with $\mathbb{E}\{\cdot\}$ denoting statistical expectation.

To this effect, when SU_i makes a decision based on the local observations, the corresponding energy Y_i can be statistically represented as follows [2]

$$Y_i = \begin{cases} \chi_{2u}^2, & \mathcal{H}_0 \\ \chi_{2u}^2(2\gamma_i), & \mathcal{H}_1 \end{cases} \tag{3}$$

where u denotes the time bandwidth product, γ_i represents the instantaneous SNR of the received signal at the SU_i, χ_{2u}^2 denotes a central chi-square distribution with $2u$ degrees of freedom, and $\chi_{2u}^2(2\gamma_i)$ represents a noncentral chi-square distribution with $2u$ degrees of freedom. Hence, the detection of PU signals can be realized by comparing Y_i with a predetermined energy threshold λ_i, which is represented as

$$\begin{cases} D_i = 1, & Y_i \geq \lambda_i \\ D_i = 0, & Y_i < \lambda_i \end{cases} \tag{4}$$

Based on the above, the probability density function (PDF) of Y_i under the two considered hypotheses is given by

$$f_{Y_i}(y) = \begin{cases} \frac{1}{2^u \Gamma(u)} y^{u-1} \exp(-\frac{y}{2}), & \mathcal{H}_0 \\ \frac{1}{2}(\frac{y}{2\gamma_i})^{\frac{u-1}{2}} \exp(-\frac{2\gamma_i + y}{2}) I_{u-1}(\sqrt{2\gamma_i y}), & \mathcal{H}_1 \end{cases} \tag{5}$$

which yields the corresponding conditional probability of false-alarm and probability of detection:

$$\hat{P}_{f_i} = \Pr\{Y_i > \lambda_i | \mathcal{H}_0\} \tag{6}$$

and

$$\hat{P}_{d_i} = \Pr\{Y_i > \lambda_i | \mathcal{H}_1\} \tag{7}$$

respectively, which yield

$$\hat{P}_{f_i} = \int_{\lambda}^{\infty} f_{Y_i|\mathcal{H}_0}(y)\, \mathrm{d}y = \frac{\Gamma\left(u, \frac{\lambda_i}{2}\right)}{\Gamma(u)} \tag{8}$$

and

$$\hat{P}_{d_i} = \int_{\lambda}^{\infty} f_{Y_i|\mathcal{H}_1}(y)\, \mathrm{d}y = Q_u\left(\sqrt{2\gamma_i}, \sqrt{\lambda_i}\right) \tag{9}$$

where $\Gamma(a)$ and $\Gamma(a, x)$ denote the Euler gamma function and the upper incomplete gamma function, respectively, $I_n(x)$ is the n^{th} order modified Bessel function of the first kind, and $Q_m(a, b)$ is the generalized Marcum $Q-$function [41].

This article has been accepted for publication in a future issue of this journal, but has not been fully edited. Content may change prior to final publication. Citation information: DOI 10.1109/TSUSC.2019.2896667, IEEE Transactions on Sustainable Computing

Since the $\hat{P}_{f_i}$ is independent of γ_i and the present signal in the $\mathcal{H}_1$ hypothesis is typically subject to non-negligible fading effects that affect the corresponding probability of detection, the unconditional probabilities of false alarm and detection are given by

$$\begin{cases} P_{f_i} = \hat{P}_{f_i} \\ P_{d_i} = \int_{\gamma} \hat{P}_{d_i}(\gamma) f(\gamma_i) \mathrm{d}\gamma \end{cases} \tag{10}$$

where $f(\gamma_i)$ denotes the SNR PDF of the statistics of the SU_i sensing channel [42]. To this effect, by specifically assuming Rayleigh distributed multipath fading and that SU_i performs local sensing independently, it follows that the average probability of detection and probability of false alarm of each antenna are expressed as [2]:

$$\begin{aligned} P_d =& e^{-\frac{\lambda}{2}} \sum_{n=0}^{u-2} \frac{\lambda^n}{n! 2^n} + \left(\frac{1+\bar{\gamma}}{\bar{\gamma}}\right)^{u-1} \\ & \times \left\{ e^{-\frac{\lambda}{2(1+\bar{\gamma})}} - e^{-\frac{\lambda}{2}} \sum_{n=0}^{u-2} \frac{\lambda^n \bar{\gamma}^n}{n! 2^n (1+\bar{\gamma})^n} \right\} \end{aligned} \tag{11}$$

and

$$P_f = \frac{\Gamma(u, \lambda/2)}{\Gamma(u)} \tag{12}$$

respectively, where $\bar{\gamma}$ denotes the corresponding average SNR.

4.2 Square-Law Selection

It is widely known that diversity receivers can significantly improve the performance of CRNs, particularly in the presence of multipath fading and shadowing effects. Based on this, square-law combining and square-law selection (SLS) techniques have been employed extensively in numerous spectrum sensing scenarios. Although the SLS combining technique is sub-optimal when compared to the former combining scheme, it is adopted in our C-CSS due to its tractability and low complexity that renders its realization straightforward. To this end, it is first recalled that SLS is based on the selection of the branch with the maximum $\gamma^{(j)}$ for each SU, namely

$$\gamma_{\mathrm{SLS}} = \max_{j=1,2,\ldots,L} \gamma^{(j)} \tag{13}$$

where L denotes the number of antennas at each SU node. Therefore, the probability of false alarm of each SU can be expressed as

$$P_{f,\mathrm{SLS}} = 1 - \Pr(\gamma_{\mathrm{SLS}} < \lambda \,|\mathcal{H}_0) \tag{14}$$

which upon use of (13) can be written as follows:

$$P_{f,\mathrm{SLS}} = 1 - \Pr(\max(\gamma^{(1)}, \gamma^{(2)}, ..., \gamma^{(L)}) < \lambda \,|\mathcal{H}_0) \tag{15}$$

which can be alternatively re-written as

$$P_{f,\mathrm{SLS}} = 1 - [1 - P_f]^L. \tag{16}$$

Likewise, the average probability of detection of each SU for the SLS scheme is expressed as

$$P_{d,\mathrm{SLS}} = 1 - [1 - P_d]^L. \tag{17}$$

4.3 Multi-User Detection

In multi-user sensing, local decisions are reported to the FC through dedicated reporting channels which are also subject to detrimental fading effects and additive noise. By letting $P_{e,i}$ denote the reporting error between the i^{th} SU and the FC and, without loss of generality, assuming that all reporting channels are independent and identically distributed, for a given γ with binary phase shift keying (BPSK), the probability of reporting error under AWGN can be expressed as

$$P_{\mathrm{e,AWGN}} = Q(\sqrt{2\gamma}) \tag{18}$$

where $Q(\cdot)$ denotes the one dimensional Gaussian $Q-$function [41]. Hence, for the case of Rayleigh distributed multipath fading, the average error rate, P_e, is given by

$$P_e = \int_{\gamma} Q(\sqrt{2\gamma}) f(\gamma) \mathrm{d}\gamma \tag{19}$$

$$= \frac{1}{\bar{\gamma}} \int_0^{\infty} Q(\sqrt{2\gamma}) e^{-\frac{\gamma}{\bar{\gamma}}} \mathrm{d}\gamma \tag{20}$$

which can be expressed in closed-form as follows

$$P_e = \frac{1}{2}\left(1 - \sqrt{\frac{\bar{\gamma}}{1+\bar{\gamma}}}\right). \tag{21}$$

Since in T-CSS, both types of decisions are sent to the FC, the imperfect false-alarm probability and detection probability can be expressed as

$$P'_{f,\mathrm{SLS,T-CSS}} = \Pr\{\mathcal{H}_1|\mathcal{H}_0\}(1-P_e) + \Pr\{\mathcal{H}_0|\mathcal{H}_0\}P_e \tag{22}$$

and

$$P'_{d,\mathrm{SLS,T-CSS}} = \Pr\{\mathcal{H}_1|\mathcal{H}_1\}(1-P_e) + \Pr\{\mathcal{H}_0|\mathcal{H}_1\}P_e \tag{23}$$

respectively, which yields

$$P'_{f,\mathrm{SLS,T-CSS}} = (1-P_e)P_{f,\mathrm{SLS}} + (1-P_{f,\mathrm{SLS}})P_e \tag{24}$$

and

$$P'_{d,\mathrm{SLS,T-CSS}} = (1-P_e)P_{d,\mathrm{SLS}} + (1-P_{d,\mathrm{SLS}})P_e \tag{25}$$

respectively.

Here, the FC combines all decisions and makes the final decision according to the hard k-out-of-n fusion rule. That is, the FC infers the presence of the PU when there exist at least k SUs that either (i) correctly claim $\mathcal{H}_1$ without an error in reporting phase (i.e., $(1-P_e)P_{d,\mathrm{SLS}}$), or (ii) falsely claim $\mathcal{H}_0$ with an error in reporting phase ($(1-P_{d,\mathrm{SLS}})P_e$). Therefore, it follows that for the case of T-CSS, the total probability of false alarm ($Q_{f,\mathrm{T-CSS}}$) and probability of detection ($Q_{d,\mathrm{T-CSS}}$) are represented as

$$Q_{f,\mathrm{T-CSS}} = \sum_{i=k}^{N} \binom{N}{i} \frac{(P'_{f,\mathrm{SLS,T-CSS}})^i}{(1-P'_{f,\mathrm{SLS,T-CSS}})^{-(N-i)}} \tag{26}$$

and

$$Q_{d,\mathrm{T-CSS}} = \sum_{i=k}^{N} \binom{N}{i} \frac{(P'_{d,\mathrm{SLS,T-CSS}})^i}{(1-P'_{d,\mathrm{SLS,T-CSS}})^{-(N-i)}} \tag{27}$$

This article has been accepted for publication in a future issue of this journal, but has not been fully edited. Content may change prior to final publication. Citation information: DOI 10.1109/TSUSC.2019.2896667, IEEE Transactions on Sustainable Computing

where $k \in 1, 2, ..., N$ and $\binom{b}{a}$ is the binomial coefficient [41].

On the contrary, in C-CSS, due to the fact that SUs only report their decisions *only* when they claim $\mathcal{H}_1$, the corresponding false-alarm and detection probabilities become

$$P'_{f,\mathrm{SLS,C-CSS}} = \Pr\{\mathcal{H}_1|\mathcal{H}_0\}(1-P_e) \quad (28)$$
$$= (1-P_e)P_{f,\mathrm{SLS}} \quad (29)$$

and

$$P'_{d,\mathrm{SLS,C-CSS}} = \Pr\{\mathcal{H}_1|\mathcal{H}_1\}(1-P_e) \quad (30)$$
$$= (1-P_e)P_{d,\mathrm{SLS}} \quad (31)$$

respectively. Thanks to the censoring technique, the unfavorable error terms due to erroneous reporting channels in (24) and (25) was filtered out in (28) and (30).

The number of transmitted decisions in the C-CSS scheme is not necessarily equal to the number of the sensing users, and the actual transmitted sensing decisions are based on two possible outcomes: i) the SUs detected falsely the presence of PU signals with probability $P_{f,\mathrm{SLS}}$, while the corresponding frequency band is idle; ii) the SUs detected correctly the presence of PU signals with probability $P_{d,\mathrm{SLS}}$, while the spectrum is actually being utilized. Therefore according to Bayes theory, the expected number of transmitted decisions in the C-CSS scheme can be determined as [7]:

$$M_C = \lceil N(P_0 P_{f,\mathrm{SLS}} + (1-P_0)P_{d,\mathrm{SLS}}) \rceil \quad (32)$$

where P_0 accounts for the probability of idle channel, and $\lceil . \rceil$ denotes the ceiling function. In this context, with C-CSS scheme, when utilizing the hard k-out-of-N fusion rule, for the total probability of detection, we need at least k users that correctly claim $\mathcal{H}_1$ without an error in reporting phase, i.e.,

$$Q_{d,\mathrm{C-CSS}} = \sum_{i=k_c}^{M_C} \binom{M_C}{i} \frac{(P'_{d,\mathrm{SLS,C-CSS}})^i}{(1-P'_{d,\mathrm{SLS,C-CSS}})^{-(M_C-i)}} \quad (33)$$

and for the total false-alarm probability, we need at least k users that falsely claim $\mathcal{H}_1$ without an error in the reporting phase, i.e.,

$$Q_{f,\mathrm{C-CSS}} = \sum_{i=k_c}^{M_C} \binom{M_C}{i} \frac{(P'_{f,\mathrm{SLS,C-CSS}})^i}{(1-P'_{f,\mathrm{SLS,C-CSS}})^{-(M_C-i)}} \quad (34)$$

where $k_c = 1, 2, ..., M_C$.

4.4 The False Alarm Bound

In this subsection, we determine the false alarm bound for the T-CSS and C-CSS schemes. It is noted here that the former sensing technique experiences a considerable sensing tail issue when the reporting channels are erroneous (subject to fading effects). However, with the aid of the aforementioned C-CSS setup, the sensing tail is ultimately eliminated. We demonstrate such phenomenon by considering 1-out-of-n fusion rule, *i.e.*, $k = k_c = 1$.

Proposition 1. *When the reporting channel is subjected to rayleigh fading with an average error rate of P_e, and as $P_f \to 0$, the false alarm for the considered T-CSS and C-CSS schemes can be represented as:*

$$Q_{f,\mathrm{T-CSS,min}} \approx NP_e + \mathcal{O}(P_e^2) \quad (35)$$

and

$$Q_{f,\mathrm{C-CSS,min}} = 0 \quad (36)$$

where $Q_{f,\mathrm{T-CSS,min}}$ and $Q_{f,\mathrm{C-CSS,min}}$ denote the minimum value of $Q_{f,\mathrm{T-CSS}}$ and $Q_{f,\mathrm{C-CSS}}$, respectively.

Proof. The proof is provided in Appendix A. □

There is a lower bound on the cooperative probability of false alarm $Q_{f,\mathrm{T-CSS}}$ in the T-CSS scheme, with a truncation error of the order $\mathcal{O}(P_e^2)$. Correspondingly, the cooperative probability of detection approaches zero when

$$Q_{f,\mathrm{T-CSS}} = Q_{f,\mathrm{T-CSS,min}}. \quad (37)$$

It merits to emphasize that $Q_{f,\mathrm{T-CSS,min}}$ increases proportionally with the number of SUs (N) and the fading severity (P_e) of the reporting channel. On the contrary, the lower bound on $Q_{f,\mathrm{C-CSS,min}}$ is practically *independent* of the number of SUs and the quality of the reporting channels. The above result is intuitive in the sense that when the characteristics of the reporting channel is severed from the perspective of the SU, refraining from voting is advantageous.

4.5 Detection Performance Trends

In CRNs, the cooperative probability of detection, $1-Q_f$, constitutes a reasonable measure of the spectrum utilization [11]. As already shown, Q_f is a function of local detection threshold (λ), the number of antennas (L), and the number of decisions i.e. M_C in C-CSS and N in T-CSS, where $M_C \leq N$. Next, we show how the aforementioned parameters affect the cooperative detection performancefor both T-CSS and C-CSS.

Lemma 1. *When N and L are fixed, the total cooperative detection probability, Q_d, and probability of false alarm, Q_f, of both T-CSS and C-CSS schemes decrease monotonically with respect to the detection threshold, since the following inequalities hold:*

$$\begin{cases} \frac{\partial Q_{d,\mathrm{T-CSS}}}{\partial \lambda} < 0 \\ \frac{\partial Q_{f,\mathrm{T-CSS}}}{\partial \lambda} < 0 \end{cases} \quad (38)$$

and

$$\begin{cases} \frac{\partial Q_{d,\mathrm{C-CSS}}}{\partial \lambda} < 0 \\ \frac{\partial Q_{f,\mathrm{C-CSS}}}{\partial \lambda} < 0 \end{cases} \quad (39)$$

Proof. The proof is provided in Appendix B. □

Using the derived representations in Section III.C, we can deduce insightful theoretical performance bounds. Specifically, it follows from (24)−(30) that

$$P'_{f,\mathrm{SLS,C-CSS}} \leq P'_{f,\mathrm{SLS,T-CSS}}, \quad (40)$$

This article has been accepted for publication in a future issue of this journal, but has not been fully edited. Content may change prior to final publication. Citation information: DOI 10.1109/TSUSC.2019.2896667, IEEE Transactions on Sustainable Computing

where the indicated equality holds only when $P_e = 0$. Likewise, from (26) and (34) and recalling that $M_C \leq N$ yields

$$Q_{f,\mathrm{C-CSS}} \leq Q_{f,\mathrm{T-CSS}}. \tag{41}$$

Thus, it is evident that although the cooperative probability of false alarm in both T-CSS and C-CSS decreases monotonically with λ, the C-CSS scheme can achieve lower probability of false alarm compared to its traditional counterpart.

Remark 1. *When L and λ are fixed, the total cooperative detection probability Q_d and probability of false alarm Q_f of both T-CSS and C-CSS schemes increase monotonically with the number of local decision results.*

This is evident by the fact that in the case of T-CSS, it is straightforwardly observed that Q_f from (32) and (34) are monotonically increasing with the number of sensing users, while the following accurate representations are also valid

$$\frac{\partial Q_{f,\mathrm{T-CSS}}}{\partial N} \approx Q_{f,\mathrm{T-CSS}}(N+1) - Q_{f,\mathrm{T-CSS}}(N) > 0 \tag{42}$$

and

$$\frac{\partial Q_{d,\mathrm{T-CSS}}}{\partial N} \approx Q_{d,\mathrm{T-CSS}}(N+1) - Q_{d,\mathrm{T-CSS}}(N) > 0. \tag{43}$$

Likewise, for the C-CSS scheme, it follows from equations (32), (34) and (33) that

$$\frac{\partial Q_{f,\mathrm{C-CSS}}}{\partial N} = \frac{\partial Q_{f,\mathrm{C-CSS}}}{\partial M_C}\frac{\partial M_C}{\partial N} > 0 \tag{44}$$

and

$$\frac{\partial Q_{d,\mathrm{C-CSS}}}{\partial N} = \frac{\partial Q_{d,\mathrm{C-CSS}}}{\partial M_C}\frac{\partial M_C}{\partial N} > 0 \tag{45}$$

which can be accurately expressed as follows:

$$\begin{aligned}\frac{\partial Q_{d,\mathrm{C-CSS}}}{\partial N} \approx &\{Q_{d,\mathrm{C-CSS}}(M_C+1) - Q_{d,\mathrm{C-CSS}}(M_C)\} \\ &\times \{P_0 P_{f,\mathrm{SLS}} + (1-P_0)P_{d,\mathrm{SLS}}\}.\end{aligned} \tag{46}$$

Notably, when λ and L are known, lower probability of false alarm can be obtained by the C-CSS scheme compared to its T-CSS counterpart, since the transmitted local decision results in C-CSS are less than those in T-CSS. Alternatively, lower energy detection threshold is required in the C-CSS scheme to reach the same target probability of detection as in T-CSS.

Lemma 2. *When N and λ are fixed, the total cooperative probability of detection Q_d and probability of false alarm Q_f increase monotonically with the number of antennas L in both T-CSS and C-CSS, where the following inequalities are valid:*

$$\begin{cases} \frac{\partial Q_{d,\mathrm{T-CSS}}}{\partial L} > 0 \\ \frac{\partial Q_{f,\mathrm{T-CSS}}}{\partial L} > 0 \end{cases} \tag{47}$$

and

$$\begin{cases} \frac{\partial Q_{d,\mathrm{C-CSS}}}{\partial L} > 0 \\ \frac{\partial Q_{f,\mathrm{C-CSS}}}{\partial L} > 0 \end{cases} \tag{48}$$

Proof. The proof is provided in Appendix C. □

It is noted that Lemma 2 verifies that the probability of detection and probability of false alarm increase with the number of antennas for fixed values of N and λ. However, the main difference between the two approaches is that lower probability of false alarm can be achieved by C-CSS.

5 Secondary Throughput

With an idle PU and no false-alarm generated with probability $P_0(1-Q_f)$, the SU throughput can be expressed as $(W-NB)\delta_0/W$, where δ_0 represents the throughput of the secondary network with idle PU. On the contrary, when the PU is active and the probability of miss-detection is $P_1(1-Q_d)$, the corresponding throughput is $(W-NB)\delta_1/W$, where δ_1 represents the throughput of the SU with active PU. Thus, the average throughput in the T-CSS scheme can be expressed as

$$\begin{aligned}R(N,L,\lambda) =& \frac{W-NB}{W}\delta_0 P_0(1-Q_f(N,L,\lambda)) \\ &+ \frac{W-NB}{W}\delta_1 P_1(1-Q_d(N,L,\lambda)).\end{aligned} \tag{49}$$

Given that the core objective of cognitive radio systems is to maximize the spectrum utilization by ensuring a smooth operation for PUs, it is evident that when sufficient protections to PUs are satisfied, such as 0.9, the first term in the right hand side of (49) becomes dominant. Thus, in T-CSS we can maximize the secondary throughput subject to a pre-defined target cooperative probability of detection according to

$$\overline{R}_{\mathrm{T-CSS}}(N,L,\lambda) \approx (1-N\alpha)(1-Q_f(N,L,\lambda)) \tag{50}$$

where $\alpha = B/W$ denotes the ratio of the occupied control bandwidth, for sending 1-bit local decision, to the overall system bandwidth. Likewise, in the case of C-CSS the normalized achievable throughput can be expressed as

$$\bar{R}_{C-\mathrm{CSS}}(M_C,L,\lambda) \approx (1-\alpha M_C)(1-Q_f(M_C,L,\lambda)) \tag{51}$$

where M_C is a function of N, as in (32). The relationship trend between the probability of detection, probability of false-alarm, and secondary throughput with N, L and λ is depicted in Table I.

TABLE 1: Effect of N, L and λ on the System Performance.

Parameters \ Performance	Q_d	Q_f	R	Interference to the PU
$\lambda \uparrow (N, L, fixed)$	↓	↓	↑	↑
$N \uparrow (\lambda, L, fixed)$	↓	↓	↑	↑
$L \uparrow (\lambda, N, fixed)$	↑	↑	↓	↓

It is recalled that one of the core aims of the analysis of the considered setup is to maximize the probability of detection and minimize the probability of false alarm. To this end, the optimal fusion rule in the minimization of the total error rate, when N and L are fixed, depends

This article has been accepted for publication in a future issue of this journal, but has not been fully edited. Content may change prior to final publication. Citation information: DOI 10.1109/TSUSC.2019.2896667, IEEE Transactions on Sustainable Computing

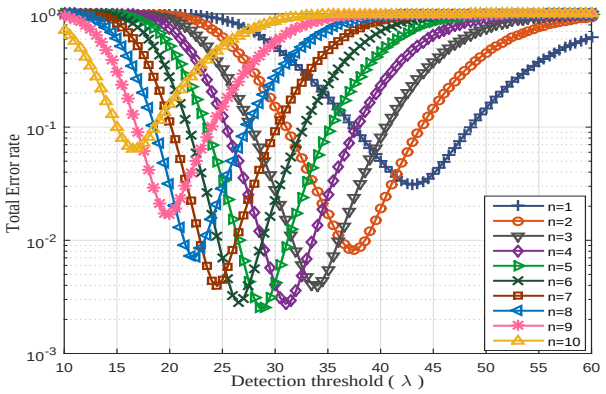

Fig. 3: Total error rate with different fusion rules for varying values of N and fixed L.

only on the detection threshold, as shown in Fig. 3. On the contrary, when L and λ are fixed, the target probability of detection is guaranteed by decreasing the level of the detection threshold (λ) and increasing the probability of false alarm. Finally, when N and λ are fixed, the probability of detection and the probability of false alarm increase proportionally with the number of antennas, which reduces the corresponding secondary throughput.

In addition, the actual number of local decisions is different in the T-CSS scheme than in C-CSS, which is related to N. Therefore, there should be an optimum balance between N, L and λ in order to achieve secondary throughput maximization while satisfying the target probability of detection. Based on the above, if we increase L, the detection threshold should be improved to ensure the target detection probability $\bar{Q}_d$ and improve the secondary throughput. To this effect, better performance can be achieved with the C-CSS scheme at a lower number of SUs, which ultimately yields reduced control bandwidth requirements. Likewise, when N, L and λ are fixed, higher secondary throughput can be achieved with the aid of the C-CSS scheme compared to the T-CSS counterpart.

5.1 Secondary Throughput Optimization

We consider the optimization problem of finding the optimal values of (N, L, λ) that maximize the secondary throughput while satisfying the condition $Q_d \geq \bar{Q}_d$, where $\bar{Q}_d$ is the minimum target detection probability which practically takes values between 0.9 and 1. According to the Neyman-Pearson criterion [43] , when N and L are fixed, the optimization problem can be formulated as follows [44]:

$$\begin{cases} \max\limits_{\lambda} \overline{R}(\lambda) = (1 - N\alpha)(1 - Q_f(\lambda)) \\ \text{s.t.} \qquad\qquad Q_d \geq \bar{Q}_d \end{cases} \tag{52}$$

By also using (39) and (52), it is readily shown that

$$\frac{\partial \overline{R}(\lambda)}{\partial \lambda} = -(1 - N\alpha)\frac{\partial Q_f(\lambda)}{\partial \lambda} > 0 \tag{53}$$

and therefore, there is a maximum point of $\overline{R}$ within the $(0, \ \lambda^{\text{opt}})$ interval, where λ^{opt} depends on the constraint in (52).

For a given N and L and following [44], the detection threshold λ_0 is selected such that $Q_d(\lambda_0) = \bar{Q}_d$. If we select a the detection threshold $\lambda_1 \leq \lambda_0$ such that $Q_d(\lambda_1) \geq Q_d(\lambda_0)$, $Q_f(\lambda_1) \geq Q_f(\lambda_0)$, and thus, $\bar{R}(\lambda_1) \leq \bar{R}(\lambda_0)$. Hence, the optimal solution to (53) can be achieved when the constraint in (52) is equality. Alternatively, the maximized secondary throughput could be achieved by maintaining PU sufficiently protected when λ_0 is selected as the detection threshold. Notably, a suboptimum spectrum utilization can be also achieved by minimizing Q_f. The detailed steps of the optimal algorithm are described as follows:

• Find the optimal detection threshold λ^{opt} for each N and L. This can be realized by using several existing algorithms, such as Newton-Raphson, Bi-Section, SECOND, to determine the root of the equation $Q_d(\lambda) = \bar{Q}_d$. In the present analysis we adopt the Newton-Raphson method as it provides a faster convergence rate compared to other algorithms [45]. Moreover, in our context, the algorithm is guaranteed to converge since $Q_d(\lambda)$ is differentiable and its partial derivative with respect to λ is monotonic (as shown in Lemma 1) [46]. It is also noted that the maximization process for both T-CSS and C-CSS schemes is rather similar. Thus, we only demonstrate the maximization of the T-CSS case. To this end, we initially let

$$g(\lambda_N^{\text{opt}}) = Q_{d,\text{T-CSS}}(\lambda_N^{\text{opt}}) - \bar{Q}_d \tag{54}$$

where the process of the Newton-Raphson algorithm is described in Algorithm 1. Based on this and with the aid

Algorithm 1 the Newton-Raphson algorithm

procedure
Step 1.1:
  Choose the tolerance $\lambda_{N,L}^{opt}(1)$
  the initial guess ε
  $i \leftarrow 1$
Step 1.2:
  if $g(\lambda_{N,L}^{opt}(i))| < \varepsilon$ **then return** stop
    otherwise goto *step 1.3*.
Step 1.3:
  Let
$\lambda_{N,L}^{opt}(i+1) = \lambda_{N,L}^{opt}(i) - g(\lambda_{N,L}^{opt}(i))/g'(\lambda_{N,L}^{opt}(i))$
  $i \leftarrow i + 1$.
  goto *step 1.2*.

of equations (17), (25) and (34), we can determine the optimal detection threshold that maximizes the secondary throughput when the target detection probability $\bar{Q}_d$ is satisfied as follows:

- Determine the corresponding local probability of false alarm $P_{f,\text{T-CSS}}^{\text{opt}}$ and the probability of detection $P_{d,\text{T-CSS}}^{\text{opt}}$ of each antenna based on (8) and (9).
- Determine the i^{th} SU probability of detection $P_{d,\text{SLS,T-CSS}}^{\text{opt}}$ and probability of false alarm

This article has been accepted for publication in a future issue of this journal, but has not been fully edited. Content may change prior to final publication. Citation information: DOI 10.1109/TSUSC.2019.2896667, IEEE Transactions on Sustainable Computing

$P^{\text{opt}}_{f,\text{SLS,T-CSS}}$ from the results of the previous step.

- Determine the corresponding probability of false alarm of CSS $Q^{\text{opt}}_{f,\text{T-CSS}}$ $(\lambda^{\text{opt}}_{N,L})$ according to (26) based on the results of the above step.
- Determine the optimal secondary throughput $R^{\text{opt}}_{\text{T-CSS}}(\lambda^{\text{opt}}_{N,L})$ according to (50).

Since the number of local decisions transmitted to the FC in C-CSS is smaller than that in T-CSS, i.e., $M_C \leq N$, the target detection probability is guaranteed when the inequality

$$P^{\text{opt}}_{d,\text{SLS,C-CSS}} \geq P^{\text{opt}}_{d,\text{SLS,T-CSS}} \tag{55}$$

is satisfied. By comparing (50) and (51), it is also noticed that the optimal detection threshold for maximizing the secondary throughput in the C-CSS scheme is smaller than that in the T-CSS scheme, namely

$$\lambda^{\text{opt}}_{\text{C-CSS}} \leq \lambda^{\text{opt}}_{\text{T-CSS}}. \tag{56}$$

To the best of the authors knowledge, the offered results have not been previously reported in the open technical literature.

6 Numerical Results

In this section, the offered analytic results are used to quantify the performance of the considered setup and develop meaningful theoretical and technical insights that will be useful in the design and deployment of CR systems. Respective results from computer simulations are also provided for verifying the validity of the offered analytic results.

Fig. 4 demonstrates the results from the analysis in Section III, where the performance of T-CSS and C-CSS is compared for different number of sensing users (N), number of antennas (L), and average SNR of the reporting channel (γ_r). Here, we assume that the average SNR of the sensing channel is (γ_s) is 10 dB, while $k = k_c = 1$, $\alpha = 0.1$, and $P_0 = 0.5$. Recall that

$$Q_{f,\text{T-CSS,min}} \approx NP_e \tag{57}$$

in T-CSS; therefore, when either N or the fading severity of the reporting channels increase, the sensing tail problem becomes more evident. The sensing tail problem is illustrated clearly in Fig. 4, where at low false alarm regions, the detection performance of the T-CSS scheme is acutely degraded, contrary to the C-CSS scheme which does not suffer from such degradation. Furthermore for the T-CSS scheme, it is shown that increasing N does not enhance the detection performance significantly, particularly in the low false alarm region, due to the dependence of the lower bound on N. Likewise, Fig. 4(b) shows that the lower bound of the probability of false alarm is independent of L, while Fig. 4(c) demonstrates the increase of the false alarm bound as γ_r decreases. Fig. 4 also shows that the detection probability in the T-CSS scheme reduces drastically to zero at the lower false alarm bound.

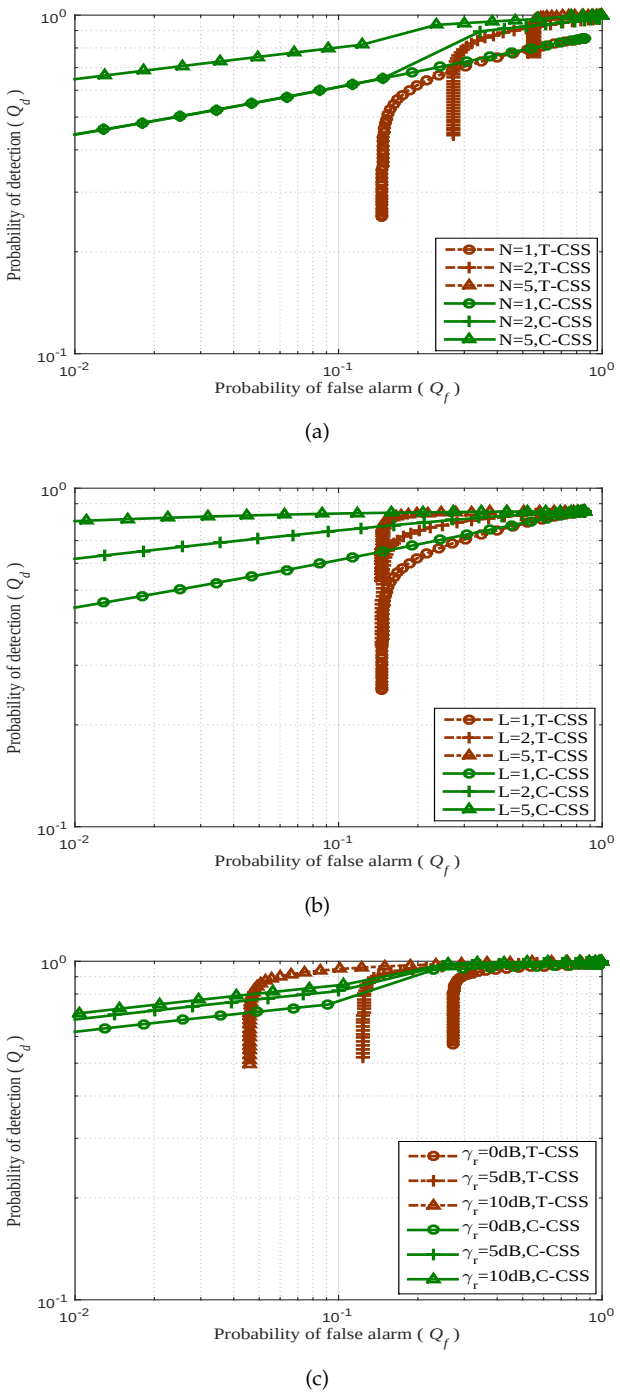

Fig. 4: Performance of C-CSS and T-CSS with: (a) different number of sensing users with L=1 and $\gamma_r = 0$dB; (b) different number of antennas with N=1 and $\gamma_r = 0$dB; (c) different SNRs γ_s of the reporting channels with L=1 and N=2.

Fig. 5 demonstrates some performance metrics versus the detection threshold for the C-CSS scheme while varying the parameters N and L. Here, we assume $k = k_c = 1$, $P_0 = 0.5$, $\alpha = 0.1$, $\gamma_r = 0$dB, and $\gamma_s = 10$dB. More specifically, Figs. 5(a) and 5(c) demonstrate that for a fixed detection threshold and as the number of sensing

This article has been accepted for publication in a future issue of this journal, but has not been fully edited. Content may change prior to final publication. Citation information: DOI 10.1109/TSUSC.2019.2896667, IEEE Transactions on Sustainable Computing

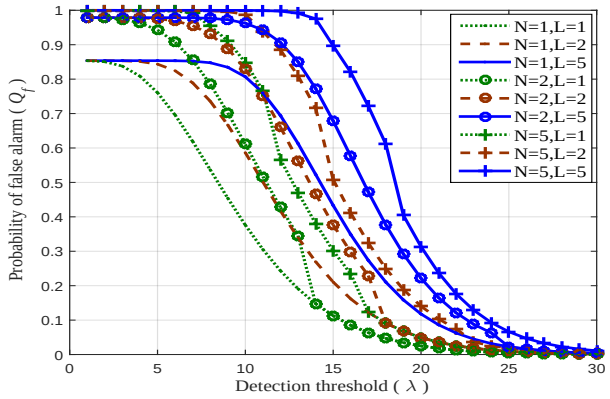

(a)

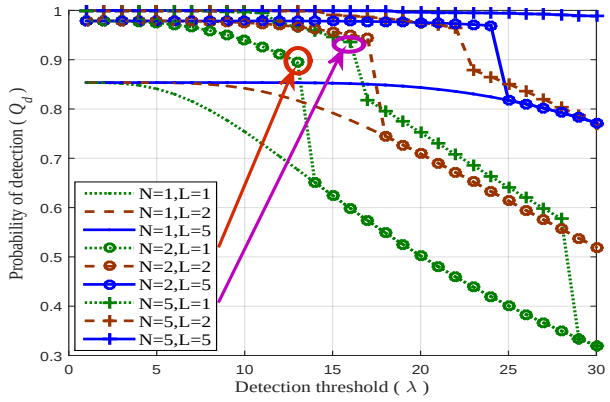

(b)

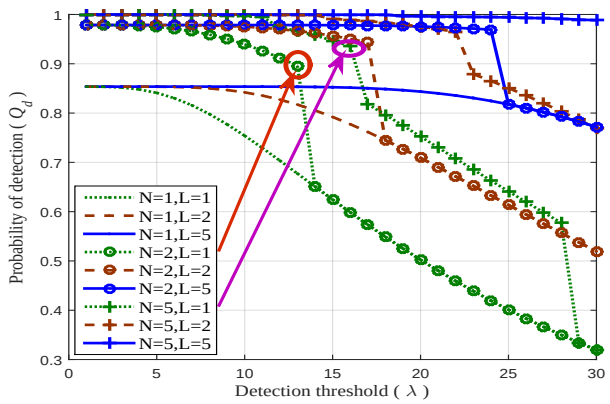

(c)

Fig. 5: The performance of C-CSS: (a) probability of false alarm; (b) normal throughput of secondary system; (c) probability of detection.

users and antennas increase, the detection and false alarm probabilities increase due to the cooperation of the multiple users. On the contrary, the secondary throughput in Fig. 5(b) degrades as N increases, due to the corresponding overhead caused by the increased multiuser cooperation. Furthermore, the secondary throughput decreases as L increases, which improves both the detection and false alarm probabilities.

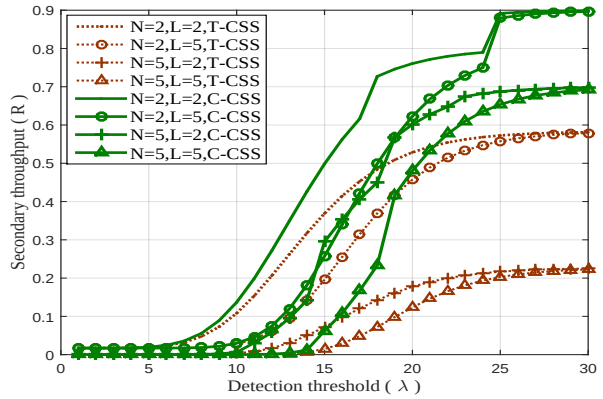

(a)

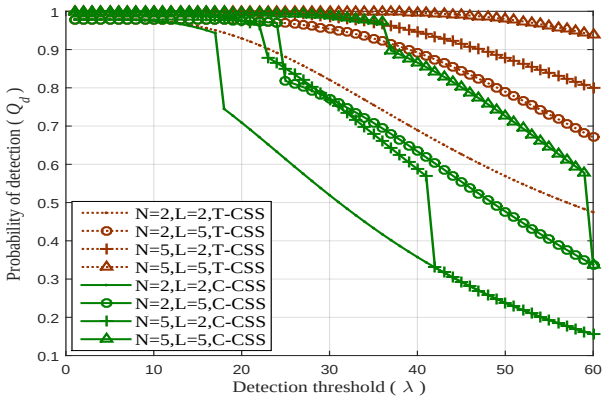

(b)

Fig. 6: The performance comparison between the C-CSS and the T-CSS schemes: (a) Normal throughput of secondary system. (b) Detection probability.

It is also observed that when N and L are kept constant and as the detection threshold λ increases, the false alarm and detection probabilities decrease, whereas the secondary throughput increases. Therefore, it is evident that larger detection threshold is required when N or L increase, demonstrating that the optimal detection threshold for maximizing the secondary throughput naturally depends on N and L. For example Fig. 5(b) demonstrates the case of $N = 2$, $L = 1$, where the maximized secondary throughput can be achieved when $\lambda = 13$, which yields a detection probability of 0.9. However, when the secondary throughput increases (e.g., $\lambda > 13$), the detection probability is considerably less than 0.9, which is also the case when $N = 5$ and $L = 1$, where the optimal detection threshold would be $\lambda = 15$.

Fig. 6 illustrates an additional comparison between the C-CSS and T-CSS schemes assuming $k = k_c = 1$, $P_0 = 0.5$, $\alpha = 0.1$, $\gamma_r = 0$dB and $\gamma_s = 10$dB. It is shown that for similar values of N and L, the C-CSS scheme outperforms the T-CSS scheme in terms of optimal secondary throughput and detection performance. For example, when $N = 5$, $L = 5$ and $\lambda = 60$,

This article has been accepted for publication in a future issue of this journal, but has not been fully edited. Content may change prior to final publication. Citation information: DOI 10.1109/TSUSC.2019.2896667, IEEE Transactions on Sustainable Computing

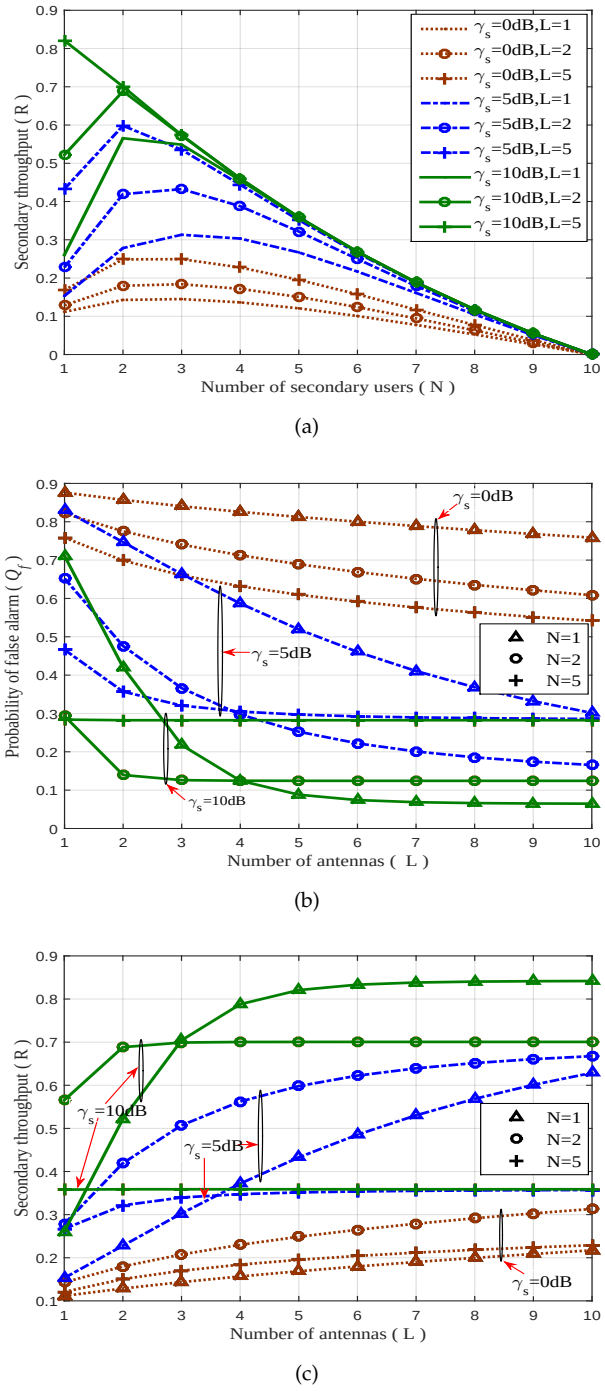

Fig. 7: Detection performance of T-CSS with optimization algorithm: (a) Secondary throughput; (b) Probability of false alarm; (c) Normal throughput of secondary system.

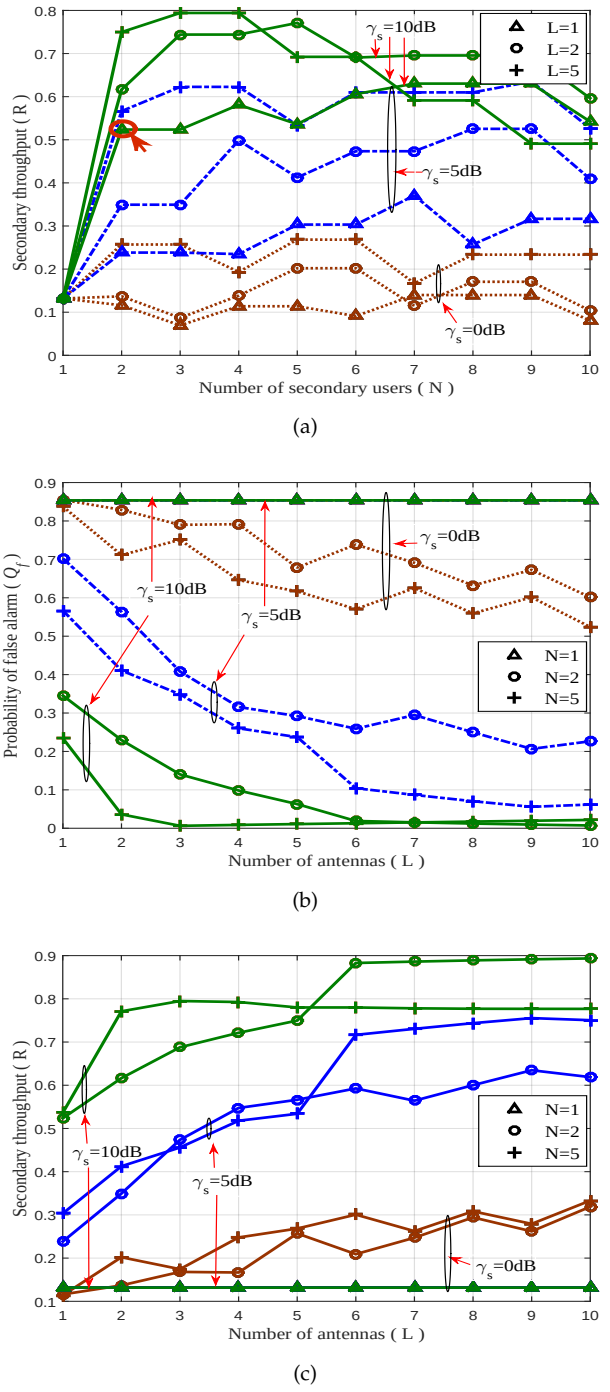

Fig. 8: Detection performance of C-CSS with optimization algorithm: (a) secondary throughput; (b) probability of false alarm; (c) normal throughput of secondary system.

the secondary throughput is increased by a factor of almost $0.7/0.2 = 3.5$, while the detection performance is enhanced by a factor of $0.9/0.6 = 1.5$, which constitutes a substantial performance improvement. In addition, for a specific target detection probability, e.g., $\bar{Q}_d = 0.9$, the required detection threshold is lower in C-CSS than in T-CSS, while higher secondary throughput can be obtained with less number of sensing users in the C-CSS scheme, which is particularly advantageous in practical realizations of CR networks.

Next, we evaluate the optimization algorithm for the secondary throughput which is employed for the T-CSS and C-CSS schemes with the assumption of SLS combining technique. To this end, Fig. 7 and Fig. 8 illustrate the detection performance of the two schemes

This article has been accepted for publication in a future issue of this journal, but has not been fully edited. Content may change prior to final publication. Citation information: DOI 10.1109/TSUSC.2019.2896667, IEEE Transactions on Sustainable Computing

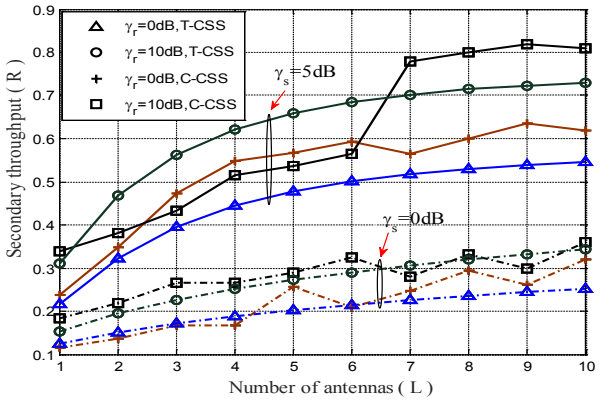

(a)

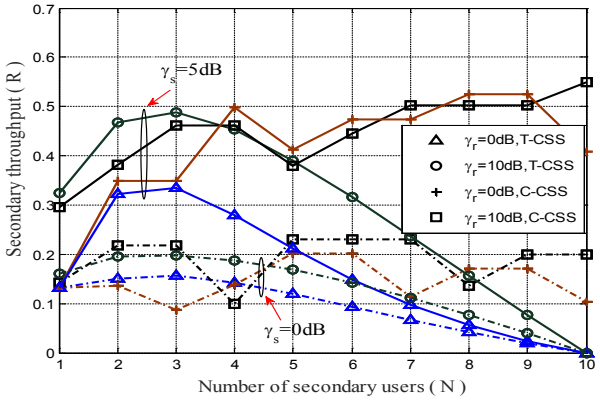

(b)

Fig. 9: Performance comparison between the C-CSS and the T-CSS schemes under different sensing channels and reporting channels with optimization algorithm for: (a) secondary throughput vs. the number of antennas ($N = 2$); (b) secondary throughput vs. the number of sensing users ($L = 2$).

under different sensing channel conditions. It is observed in Fig. 7(a) that the secondary throughput in the T-CSS exhibits a concave shape as N varies. This is in fact due to the effect of the involved cooperation, where the performance of the T-CSS scheme outperforms the single spectrum sensing when N is particularly low. Nevertheless, as N increases, the bandwidth required to send the local decisions also increases, which in turn reduces the respective secondary throughput $\bar{R}^{\text{opt}}$.

However, the secondary throughput in the C-CSS scheme plateaus as N grows, as shown in Fig. 8(c). Furthermore, comparing Fig. 7(c) with Fig. 8(c), we observe that the secondary throughput in C-CSS grows more rapidly with respect to N (especially when the number of antennas is small). For example, when $\gamma_s = 10$dB and $L = 2$, the secondary throughput increases from 0.5 to 0.7 in the T-CSS scheme, whereas it increases from 0.1 to 0.6 in the C-CSS scheme. This observation becomes even more evident as the channel conditions deteriorates, i.e., when $\gamma_s \to -\infty$ dB. It also merits to allude that for $N > 1$, the secondary throughput in the C-CSS scheme increases with respect to the number of antennas regardless of the corresponding sensing channel conditions.

Finally, Fig. 9 illustrates the optimized secondary throughput for the T-CSS and C-CSS schemes with different sensing channels and reporting channels. As shown, larger secondary throughput can be achieved in the case of C-CSS with smaller N and L. In Fig. 9(a), as parameter L increases, the optimized throughput for both T-CSS and C-CSS depicts a non-decreasing function, where the C-CSS scheme achieves considerably larger values with a faster trend. As $L \to \infty$, the secondary throughput plateaus. In Fig. 9(b), as parameter N increases, the optimized throughput for T-CSS depicts a concave trend, whereby as $N \to \infty$, the secondary throughput tends to zero. On other hand, as parameter N increases, the optimized throughput for C-CSS depicts a non-decreasing function that plateaus as $N \to \infty$.

7 Conclusion

We introduced a censor-based cooperative spectrum sensing approach using multiple antenna nodes that operates in realistic communication scenarios with imperfect sensing and reporting channel conditions. Novel analytic expressions were derived for the corresponding probabilities of detection and probabilities of false-alarm as well as for the secondary throughput in both T-CSS and C-CSS schemes. Capitalizing on this, we determined the relationship between the number of sensing users, the number of antennas and the detection thresholds. In addition, a lower bound for the cooperative false alarm was derived for the T-CSS and based on the Neyman-Pearson criterion, we proposed an optimization algorithm for maximizing the secondary throughput. Furthermore, it was shown that the considered C-CSS schemes provides a solution to the critical sensing tail problem. Numerous useful insights were developed throughout the respective analysis, which are expected to be useful in future designs and deployment of efficient cognitive radio networks.

Appendix A
Proof of Proposition 1

By substituting (16) and (24) into (26), and then differentiating (26) one obtains

$$\frac{\partial Q_{f,\text{T-CSS}}}{\partial P_f} = -N[1 - P_e - (1-2P_e)(1-[1-P_f]^L)^{N-1}] \times (-1)(1-2P_e)L[1-P_f]^{L-1} \tag{58}$$

which can be equivalently expressed as

$$\frac{\partial Q_{f,\text{T-CSS}}}{\partial P_f} = LN(1-2P_e)[1-P_f]^{L-1} \times [1 - P_e - (1-2P_e)(1-[1-P_f]^L)^{N-1}]. \tag{59}$$

This article has been accepted for publication in a future issue of this journal, but has not been fully edited. Content may change prior to final publication. Citation information: DOI 10.1109/TSUSC.2019.2896667, IEEE Transactions on Sustainable Computing

Since the error probability is practically no more than $1/2$, equation (35) satisfies the inequality

$$\frac{\partial Q_{f,\mathrm{T-CSS}}}{\partial P_f} \geq 0. \tag{60}$$

It is evident that $Q_{f,\mathrm{T-CSS}}$ is monotonically increasing with respect to P_f. Hence, the minimum value of $Q_{f,\mathrm{T-CSS}}$ is obtained when $P_f = 0$, yielding

$$Q_{f,\mathrm{T-CSS,min}} = \lim_{P_f \to 0} Q_{f,\mathrm{T-CSS}} \tag{61}$$

$$= 1 - (1 - P_e)^N. \tag{62}$$

Using the binomial expansion of $(1 + (-P_e))^N$, and truncating to the first term, we obtain

$$Q_{f,\mathrm{T-CSS,min}} \approx NP_e + \mathcal{O}(P_e^2). \tag{63}$$

In the case of C-CSS, by first substituting (16) and (28) into (34), and then differentiating (34) with respect to P_f, yields

$$\frac{\partial Q_{f,\mathrm{C-CSS}}}{\partial P_f} \approx LM_C(1 - P_e)[1 - P_f]^{L-1} \times \{(1 - (1 - P_e)(1 - [1 - P_f]^L))\}^{M_C} \tag{64}$$

which leads to

$$\frac{\partial Q_{f,\mathrm{C-CSS}}}{\partial P_f} > 0 \tag{65}$$

and thus, the minimum value of $Q_{f,\mathrm{C-CSS}}$ is given by

$$Q_{f,\mathrm{C-CSS,min}|P_f=0} = 0 \tag{66}$$

which completes the proof.

Appendix B
Proof of Lemma 1

Assuming $P_e < 0.5$ in the T-CSS scheme, from (27), the derivative of $Q_{d,\mathrm{T-CSS}}$ with respect to the threshold λ is represented as

$$\frac{\partial Q_{d,\mathrm{T-CSS}}}{\partial \lambda} = \frac{\partial Q_{d,\mathrm{T-CSS}}}{\partial P'_{d,\mathrm{SLS,T-CSS}}} \frac{\partial P'_{d,\mathrm{SLS,T-CSS}}}{\partial P_{d\_\mathrm{Rayleigh}}} \frac{\partial P_{d\_\mathrm{Rayleigh}}}{\partial \lambda} \tag{67}$$

which after some algebraic manipulations yields the following analytic representations

$$\frac{\partial Q_{d,\mathrm{T-CSS}}}{\partial P'_{d,\mathrm{SLS,T-CSS}}} = N\binom{N-1}{k-1} \frac{(P'_{d,\mathrm{SLS,T-CSS}})^N}{(1 - P'_{d,\mathrm{SLS,T-CSS}})^{k-N}} > 0 \tag{68}$$

and

$$\frac{\partial P'_{d,\mathrm{SLS,T-CSS}}}{\partial P_{d\_\mathrm{Rayleigh}}} = \frac{\partial P'_{d,\mathrm{SLS,T-CSS}}}{\partial P_{d,\mathrm{SLS}}} \frac{\partial P_{d,\mathrm{SLS}}}{\partial P_{d\_\mathrm{Rayleigh}}} \tag{69}$$

$$= \frac{L(1 - 2P_e)}{(1 - P_{d\_\mathrm{Rayleigh}})^{1-L}} \tag{70}$$

$$> 0 \tag{71}$$

as well as

$$P_{d\_\mathrm{AWGN}} = \frac{1}{\sqrt{2\gamma}} \int_{\sqrt{\lambda}}^{\infty} x^{\mu} e^{-\frac{x^2+2\gamma}{2}} I_{u-1}(\sqrt{2\gamma x})\mathrm{d}x \tag{72}$$

and

$$\frac{\partial P_{d\_\mathrm{Rayleigh}}}{\partial P_\lambda} = \int_{\sqrt{\lambda}}^{\infty} \frac{\partial P_{d\_\mathrm{AWGN}}}{\partial P_\lambda} f_\gamma(x)\mathrm{d}x \tag{73}$$

$$= \int_{\sqrt{\lambda}}^{\infty} \frac{\lambda^{\frac{u-1}{2}} I_{u-1}(\sqrt{2\gamma\lambda})}{2(\sqrt{2\gamma})^{\frac{u-1}{2}} e^{\frac{\lambda+2\gamma}{2}}} f_\gamma(x)\mathrm{d}x \tag{74}$$

$$< 0. \tag{75}$$

Substituting the above representations in (67), it follows that

$$\frac{\partial Q_{d,\mathrm{T-CSS}}}{\partial \lambda} < 0. \tag{76}$$

Likewise, from (26) it follows that

$$\frac{\partial Q_{f,\mathrm{T-CSS}}}{\partial \lambda} = \frac{\partial Q_{f,\mathrm{T-CSS}}}{\partial P'_{f,\mathrm{SLS,T-CSS}}} \frac{\partial P'_{f,\mathrm{SLS,T-CSS}}}{\partial P_f} \frac{\partial P_f}{\partial \lambda} \tag{77}$$

and

$$\frac{\partial Q_{f,\mathrm{T-CSS}}}{\partial P'_{f,\mathrm{SLS,T-CSS}}} = N\binom{N-1}{k-1} \frac{(P'_{f,\mathrm{SLS,T-CSS}})^N}{(1 - P'_{f,\mathrm{SLS,T-CSS}})^{k-N}} \tag{78}$$

which yields

$$\frac{\partial Q_{f,\mathrm{T-CSS}}}{\partial P'_{f,\mathrm{SLS,T-CSS}}} > 0. \tag{79}$$

Also,

$$\frac{\partial P'_{f,\mathrm{SLS,T-CSS}}}{\partial P_f} = \frac{\partial P'_{f,\mathrm{SLS,T-CSS}}}{\partial P_{f,\mathrm{SLS}}} \frac{\partial P_{f,\mathrm{SLS}}}{\partial P_f} \tag{80}$$

$$= L(1 - 2P_e)[1 - P_f]^{L-1} \tag{81}$$

$$> 0 \tag{82}$$

and

$$\frac{\partial P_f}{\partial \lambda} = -\frac{\lambda^{u-1}}{2^u \Gamma(u)} e^{-\frac{\lambda}{2}} < 0 \tag{83}$$

which upon using (77)–(83), it readily follows that

$$\frac{\partial Q_{f,\mathrm{T-CSS}}}{\partial \lambda} < 0. \tag{84}$$

For the C-CSS scheme, using (34) and (33) yields

$$\frac{\partial Q_{d,\mathrm{C-CSS}}}{\partial \lambda} = \binom{M_C - 1}{k_c - 1} \frac{M_C \left(P'_{d,\mathrm{SLS,C-CSS}}\right)^{M_C}}{(1 - P'_{d,\mathrm{SLS,C-CSS}})^{k_c - M_C}} \times L(1 - P_e)[1 - P_d]^{L-1} \frac{\partial P_{d\_\mathrm{Rayleigh}}}{\partial \lambda} \tag{85}$$

and

$$\frac{\partial Q_{f,\mathrm{C-CSS}}}{\partial \lambda} = \binom{M_C - 1}{k_c - 1} \frac{M_C \left(P'_{f,\mathrm{SLS,C-CSS}}\right)^{M_C}}{(1 - P'_{f,\mathrm{SLS,C-CSS}})^{k_c - M_C}} \times L(1 - P_e)[1 - P_f]^{L-1} \frac{\partial P_f}{\partial \lambda} \tag{86}$$

where $\binom{b}{a}$ denotes the binomial coefficient in [41]. Therefore, by substituting (73) into (85), it follows that

$$\frac{\partial Q_{d,\mathrm{C-CSS}}}{\partial \lambda} < 0 \tag{87}$$

This article has been accepted for publication in a future issue of this journal, but has not been fully edited. Content may change prior to final publication. Citation information: DOI 10.1109/TSUSC.2019.2896667, IEEE Transactions on Sustainable Computing

and by substituting (83) into (86) one obtains

$$\frac{\partial Q_{f,\mathrm{C-CSS}}}{\partial \lambda} < 0 \tag{88}$$

which completes the proof.

APPENDIX C
PROOF OF LEMMA 2

With the aid of (17), (25) and (27) in the T-CSS scheme, it follows that

$$\frac{\partial Q_{d,\mathrm{T-CSS}}}{\partial L} = \frac{\partial Q_{d,\mathrm{T-CSS}}}{\partial P'_{d,\mathrm{SLS,T-CSS}}} \frac{\partial P'_{d,\mathrm{SLS,T-CSS}}}{\partial P_{d,\mathrm{SLS}}} \frac{\partial P_{d,\mathrm{SLS}}}{\partial L} \tag{89}$$

where

$$\frac{\partial P_{d,\mathrm{SLS}}}{\partial L} = -[1-P_d]^L \ln[1-P_d] > 0. \tag{90}$$

Based on this and using (68), (69), (89) and (90) yields

$$\frac{\partial Q_{d,\mathrm{T-CSS}}}{\partial L} > 0. \tag{91}$$

Likewise,

$$\frac{\partial Q_{f,\mathrm{T-CSS}}}{\partial L} = \frac{\partial Q_{f,\mathrm{T-CSS}}}{\partial P'_{f,\mathrm{SLS,T-CSS}}} \frac{\partial P'_{f,\mathrm{SLS,T-CSS}}}{\partial P_{f,\mathrm{SLS}}} \frac{\partial P_{f,\mathrm{SLS}}}{\partial L} \tag{92}$$

whereas

$$\frac{\partial P'_{f,\mathrm{SLS,T-CSS}}}{\partial P_{f,\mathrm{SLS}}} = L(1-2P_e) > 0 \tag{93}$$

and

$$\frac{\partial P_{f,\mathrm{SLS}}}{\partial L} = -[1-P_f]^L \ln[1-P_f] > 0. \tag{94}$$

Hence, with the aid of (79), (92), (93) and (94), one obtains

$$\frac{\partial Q_{f,\mathrm{T-CSS}}}{\partial L} > 0. \tag{95}$$

Finally, for the C-CSS scheme, it readily follows that

$$\frac{\partial Q_{d,\mathrm{C-CSS}}}{\partial L} = \frac{\partial Q_{d,\mathrm{C-CSS}}}{\partial P'_{d,\mathrm{SLS,C-CSS}}} \frac{\partial P'_{d,\mathrm{SLS,C-CSS}}}{\partial P_{d,\mathrm{SLS}}} \frac{\partial P_{d,\mathrm{SLS}}}{\partial L} \tag{96}$$

which can be expressed in closed-form as follows

$$\frac{\partial Q_{d,\mathrm{C-CSS}}}{\partial L} = M_C \binom{M_C-1}{k_c-1} \frac{\left(P'_{d,\mathrm{SLS,C-CSS}}\right)^{M_C}}{\left(1-P'_{d,\mathrm{SLS,C-CSS}}\right)^{k_c-M_C}} \times (1-P_e) \times \frac{\partial P_{d,\mathrm{SLS}}}{\partial L}. \tag{97}$$

Likewise,

$$\frac{\partial Q_{f,\mathrm{C-CSS}}}{\partial L} = \frac{\partial Q_{f,\mathrm{C-CSS}}}{\partial P'_{f,\mathrm{SLS,C-CSS}}} \frac{\partial P'_{f,\mathrm{SLS,C-CSS}}}{\partial P_{f,\mathrm{SLS}}} \frac{\partial P_{f,\mathrm{SLS}}}{\partial L} \tag{98}$$

which can be expressed by the following closed-form representation

$$\frac{\partial Q_{f,\mathrm{C-CSS}}}{\partial L} = M_C \binom{M_C-1}{k_c-1} \frac{\left(P'_{f,\mathrm{SLS,C-CSS}}\right)^{M_C}}{\left(1-P'_{f,\mathrm{SLS,C-CSS}}\right)^{k_c-M_C}} \times (1-P_e) \times \frac{\partial P_{f,\mathrm{SLS}}}{\partial L} \tag{99}$$

which upon substitution of (90) into (97) and (94) into (99), it follows that

$$\frac{\partial Q_{d,\mathrm{C-CSS}}}{\partial L} > 0 \tag{100}$$

and

$$\frac{\partial Q_{f,\mathrm{C-CSS}}}{\partial L} > 0 \tag{101}$$

respectively, and thus, completing the proof.

ACKNOWLEDGEMENT

This work was supported in part by the National Natural Science Foundation of China (Grant No. 61672373), the Scientific and Technological Innovation Programs of Higher Education Institutions in Shanxi (Grant No. 201802090), the Program of One hundred Talented People of Shanxi Province, the Scientific and Technology Innovation Program of Shanxi Province (Grant No. 201705D131025), Project of Collaborative Innovation Center of Internet+3D Printing in Shanxi Province, The Key Innovation Team of the 1331 Project of Shanxi Province, by the Khalifa University Research KU Research Center for Cyber-Physical Systems under Grant No. 8474000137 and by Khalifa University under Grant No. 8474000122.

REFERENCES

[1] I. F. Akyildiz, W. Y. Lee, M. C. Vuran, and S. Mohanty, "Next generation/dynamic spectrum access/cognitive radio wireless networks: A survey," *Elsevier Comput. Netw.*, vol. 50, no. 13, pp. 2127–2159, 2006.

[2] L. Khaled Ben and W. Zhang, "Cooperative communications for cognitive radio networks," *Proc. IEEE*, vol. 97, no. 5, pp. 878–893, May. 2009.

[3] W. Zhang, R. Mallik and L. Khaled Ben, "Optimization of cooperative spectrum sensing with energy detection in cognitive radio networks," *IEEE Trans. Wireless Commun.*, vol. 8, no. 12, pp. 5761–5766, Dec. 2009.

[4] C. Rago, P. Willett, and Y. B. Shalom, "Censoring sensors: a low-communication-rate scheme for distributed detection," *IEEE Trans. Aerosp. Electron. Syst.*, vol. 32, no. 2, pp. 554–568, Apr. 1996.

[5] R. Jiang and B. Chen, "Fusion of censored decisions in wireless sensor networks," *IEEE Trans. Wireless Commun.*, vol. 4, no. 6, pp. 2668–2673, Nov. 2005.

[6] S. Yiu and R. Schober, "Nonorthogonal transmission and noncoherent fusion of censored decisions," *IEEE Trans. Veh. Technol.*, vol. 58, no. 1, pp. 263–273, Jan. 2009.

[7] C. Sun, W. Zhang, and L. Khaled Ben, "Cooperative spectrum sensing for cognitive radios under bandwidth constraints," in *2007 IEEE Wireless Communications and Networking Conference*. IEEE, 2007, pp. 1–5.

[8] G. Ganesan and Y. Li, "Cooperative spectrum sensing in cognitive radio, Part I: Two user networks," *IEEE Trans. Wireless Commun.*, vol. 6, no. 6, pp. 2204–2213, Jun. 2007.

This article has been accepted for publication in a future issue of this journal, but has not been fully edited. Content may change prior to final publication. Citation information: DOI 10.1109/TSUSC.2019.2896667, IEEE Transactions on Sustainable Computing

[9] G. Ganesan and Y. Li, "Cooperative spectrum sensing in cognitive radio, Part II: Multiuser networks," *IEEE Trans. Wireless Commun.*, vol. 6, no. 6, pp. 2214–2222, Jun. 2007.

[10] A. Ghasemi and E. Sousa, "Collaborative spectrum sensing for opportunistic access in fading environments," in *First IEEE International Symposium on New Frontiers in Dynamic Spectrum Access Networks, 2005. DySPAN 2005.* IEEE, pp. 131–136.

[11] A. Ghasemi and E. S. Sousa, "Opportunistic spectrum access in fading channels through collaborative sensing," *Journal of Communications*, vol. 2, no. 2, pp. 71–82, Mar. 2007.

[12] A. Ghasemi and E. S. Sousa, "Spectrum sensing in cognitive radio networks: the cooperation-processing tradeoff," *Wireless Communications and Mobile Computing*, vol. 7, no. 9, pp. 1049–1060, Nov. 2007.

[13] S. Zheng, Y. C. Liang, P. Y. Kam, and A. T. Hoang, "Cross-layered design of spectrum sensing and MAC for opportunistic spectrum access," in *2009 IEEE Wireless Communications and Networking Conference*. IEEE, Apr. 2009, pp. 1–6.

[14] Y. Zeng and Y. C. Liang, "Spectrum-sensing algorithms for cognitive radio based on statistical covariances," *IEEE Trans. Veh. Technol.*, vol. 58, no. 4, pp. 1804–1815, May. 2009.

[15] Y. Selen, H. Tullberg, and J. Kronander, "Sensor selection for cooperative spectrum sensing," in *2008 3rd IEEE Symposium on New Frontiers in Dynamic Spectrum Access Networks,*. IEEE, Oct. 2008, pp. 1–11.

[16] V. Bhargava, "Adaptive wireless access system design for cognitive radio networks," in *2007 IEEE Radio and Wireless Symposium*. IEEE, Jan. 2007, pp. 5–6.

[17] W. Y. Lee and I. F. Akyildiz, "Optimal spectrum sensing framework for cognitive radio networks," *IEEE Trans. Wireless Commun.*, vol. 7, no. 10, pp. 3845–3857, Oct. 2008.

[18] Y. C. Liang, Y. H. Zeng, E. Peh, and Anh Tuan Hoang, "Sensing-throughput tradeoff for cognitive radio networks," *IEEE Trans. Wireless Commun.*, vol. 7, no. 4, pp. 1326–1337, Apr. 2008.

[19] J. Shen, T. Jiang, S. Liu, and Z. Zhang, "Maximum channel throughput via cooperative spectrum sensing in cognitive radio networks," *IEEE Trans. Wireless Commun.*, vol. 8, no. 10, pp. 5166–5175, Oct. 2009.

[20] Y. Pei, A. T. Hoang, and Y. C. Liang, "Sensing-throughput tradeoff in cognitive radio networks: how frequently should spectrum sensing be carried out?" in *2007 IEEE 18th International Symposium on Personal, Indoor and Mobile Radio Communications*. IEEE, 2007, pp. 1–5.

[21] E. Peh, Y. C. Liang, Y. L. Guan, and Y. Zeng, "Optimization of cooperative sensing in cognitive radio networks: a sensing-throughput tradeoff view," *IEEE Trans. Veh. Technol.*, vol. 58, no. 9, pp. 5294–5299, Nov. 2009.

[22] A. Dehghani Firouzabadi and A. M. Rabiei, "Sensing-throughput optimisation for multichannel cooperative spectrum sensing with imperfect reporting channels," *IET Communications*, vol. 9, no. 18, pp. 2188–2196, 2015.

[23] M. Zheng, L. Chen, W. Liang, H. Yu, and J. Wu, "Energy-efficiency maximization for cooperative spectrum sensing in cognitive sensor networks," *IEEE Transactions on Green Communications and Networking*, vol. 1, no. 99, pp. 29–39, 2017.

[24] Y. Liu, S. Xie, R. Yu, Y. Zhang, and C. Yuen, "An efficient mac protocol with selective grouping and cooperative sensing in cognitive radio networks," *IEEE Transactions on Vehicular Technology*, vol. 62, no. 8, pp. 3928–3941, 2013.

[25] R. Deng, J. Chen, C. Yuen, P. Cheng, and Y. Sun, "Energy-efficient cooperative spectrum sensing by optimal scheduling in sensor-aided cognitive radio networks," *IEEE Transactions on Vehicular Technology*, vol. 61, no. 2, pp. 716–725, 2012.

[26] M. Zheng, W. Liang, H. Yu, and M. Song, "Smcss: A quick and reliable cooperative spectrum sensing scheme for cognitive industrial wireless networks," *IEEE Access*, vol. 4, no. 99, pp. 9308–9319, 2017.

[27] H. Li, H. Dai, and C. Li, "Collaborative quickest spectrum sensing via random broadcast in cognitive radio systems," *IEEE Transactions on Wireless Communications*, vol. 9, no. 7, pp. 2338–2348, 2010.

[28] G. Noh, H. Wang, J. Jo, B. H. Kim, and D. Hong, "Reporting order control for fast primary detection in cooperative spectrum sensing," *IEEE Transactions on Vehicular Technology*, vol. 60, no. 8, pp. 4058–4063, 2011.

[29] W. Zhang, R. Mallik and L. Khaled Ben, "Cooperative spectrum sensing optimization in cognitive radio networks," in *2008 IEEE International Conference on Communications*. IEEE, 2008, pp. 3411–3415.

[30] A. A. A. Boulogeorgos, N. D. Chatzidiamantis, and G. K. Karagiannidis, "Spectrum sensing under hardware constraints," pp. 1–30, Oct. 2015. [Online]. Available: https://arxiv.org/pdf/1510.06527v1.pdf

[31] J. W. Lee, "Cooperative spectrum sensing scheme over imperfect feedback channels," *IEEE Commun. Lett.*, vol. 17, no. 6, pp. 1192–1195, Jun. 2013.

[32] D. Benevides, M. Elkashlan, and P. Yeoh, "Dual-hop cooperative spectrum sharing systems with multi-primary users and multi-secondary destinations over nakagami-m fading," in *IEEE Int. Symposium Personal, Indoor and Mobile Radio Commun.*, Sydney, 2012, pp. 1577–1581.

[33] B. Selim, O. Alhussein, S. Muhaidat, G. K. Karagiannidis, and J. Liang, "Modeling and analysis of wireless channels via the mixture of gaussian distribution," *IEEE Trans. Veh. Technol.*, vol. 65, no. 10, pp. 8309–8321, Oct. 2016.

[34] T. Q. Duong, D. B. da Costa, M. Elkashlan, and Vo Nguyen Quoc Bao, "Cognitive amplify-and-forward relay networks over Nakagami-m fading," *IEEE Trans. Veh. Technol.*, vol. 61, no. 5, pp. 2368–2374, 2012.

[35] P. C. Sofotasios, E. Rebeiz, L. Zhang, T. A. Tsiftsis, D. Cabric, and S. Freear, "Energy detection based spectrum sensing over \kappa-\mu and \kappa-\mu extreme fading channels," *IEEE Trans. Veh. Technol.*, vol. 62, no. 3, pp. 1031–1040, Mar. 2013.

[36] O. Altrad, S. Muhaidat, A. A.Dweik, A. Shami, and P. D. Yoo, "Opportunistic spectrum access in cognitive radio networks under imperfect spectrum sensing," *IEEE Trans. Veh. Technol.*, vol. 63, no. 2, pp. 920–925, Feb. 2014.

[37] A. A. Hammadi, O. Alhussein, P. C. Sofotasios, S. Muhaidat, M. Al Qutayri, S. Al Araji, G. K. Karagiannidis, and J. Liang, "Unified analysis of cooperative spectrum sensing over composite and generalized fading channels," *IEEE Trans. Veh. Technol.*, vol. 65, no. 9, pp. 6949–6961, Sep. 2016.

[38] M. L. Li, C. W. Yuan, L. Li, and R. Yang, "Performance analysis and optimization of cooperative spectrum sensing for maximizing secondary throughput," *Chinese Journal on Communications*, vol. 32, no. 2, pp. 53–60, Feb. 2011.

[39] M. Li, A. Wang, and J. S. Pan, *Cognitive wireless networks using the CSS technology*. Springer, 2016.

[40] S. Q. Liu, B. J. Hu, and X. Y. Wang, "Hierarchical cooperative spectrum sensing based on double thresholds energy detection," *IEEE Communications Letters*, vol. 16, no. 7, pp. 1096–1099, 2012.

[41] I. Gradshteyn and I. Ryzhik, *Table of Integrals, Series, and Products*, 2014.

[42] J. G. Proakis, *Digital Communications*, 4th ed. McGraw-Hill, 2001.

[43] J. Shen, S. Liu, L. Zeng, G. Xie, J. Gao, and Y. Liu, "Optimisation of cooperative spectrum sensing in cognitive radio network," *IET Communications*, vol. 3, no. 7, pp. 1170–1178, Aug. 2009.

[44] M.-L. Li, C.-W. Yuan, L. Lin, and R.-Z. Yang, "Analysis of secondary throughput and optimization in cooperative spectrum sensing," *The Journal of China Universities of Posts and Telecommunications*, vol. 18, no. 4, pp. 39–44, 2011.

[45] S. Boyd and L. Vandenberghe, *Convex Optimization*. Cambridge Univ. Press, 2004.

[46] S. R. Victor and e. . Semyon, V, *A Theoretical Introduction to Numerical Analysis* . Chapman and Hall/CRC, 2006.

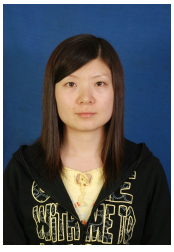

Meiling Li received her M.S. and Ph. D in Signal and Information Processing from Beijing University of Posts and Telecommunications (BUPT) in 2007 and 2012, respectively. She is now an associate professor in the School of Electronics Information Engineering, Taiyuan University of Science and Technology (TYUST), China. Her research interests include cognitive radio, cooperative communications, NOMA and PLS technology.

This article has been accepted for publication in a future issue of this journal, but has not been fully edited. Content may change prior to final publication. Citation information: DOI 10.1109/TSUSC.2019.2896667, IEEE Transactions on Sustainable Computing

Omar Alhussein (S'14) received the B.Sc. degree in communications engineering from Khalifa University, Abu Dhabi, United Arab Emirates, in 2013 and the M.A.Sc. degree in engineering science from Simon Fraser University, Burnaby, BC, Canada, in 2015. He is currently working towards the Ph.D. degree in the Broadband Communications Research Laboratory, University of Waterloo, Waterloo, ON, Canada. From January 2014 to May 2014, he was a Research Assistant with the Etisalat BT Innovation Centre (EBTIC), Khalifa University. From May 2014 to September 2015, he was with the Multimedia Communications Laboratory, Simon Fraser University. His research interests are in areas spanning software defined networking, network virtualization, wireless communications, and machine learning.

Paschalis C. Sofotasios (S'07-M'12-SM'16) was born in Volos, Greece, in 1978. He received the M.Eng. degree from Newcastle University, U.K., in 2004, the M.Sc. degree from the University of Surrey, U.K., in 2006, and the Ph.D. degree from the University of Leeds, U.K., in 2011. His M.Sc. studies were funded by a scholarship from UK-EPSRC, and his Doctoral studies were sponsored by UK-EPSRC and Pace plc. He has held academic positions at the University of Leeds, the University of California, Los Angeles, CA, USA, Aristotle University of Thessaloniki, Greece, Tampere University of Technology, Finland, and Khalifa University of Science and Technology, where he is an Assistant Professor in the Department of Electrical and Computer Engineering. His research interests are in the broad areas of digital and optical wireless communications as well as topics relating to mathematics and statistics.

Dr. Sofotasios serves as a regular reviewer for several international journals and has been a member of the Technical Program Committee of numerous IEEE conferences. He was a co-recipient of the Best Paper Award at ICUFN '13. He currently serves as an Editor of the IEEE COMMUNICATIONS LETTERS and he has received an Exemplary Reviewer Award by the IEEE COMMUNICATIONS LETTERS in 2012 and by the IEEE TRANSACTIONS ON COMMUNICATIONS in 2015 and 2016.

Sami Muhaidat (S'01-M'08-SM'11) received the Ph.D. degree in electrical and computer engineering from the University of Waterloo, Waterloo, ON, Canada, in 2006. From 2007 to 2008, he was an NSERC Post-Doctoral Fellow with the Department of Electrical and Computer Engineering, University of Toronto, Toronto, ON, Canada. From 2008 to 2012, he was an Assistant Professor with the School of Engineering Science, Simon Fraser University, Burnaby, BC, Canada. He is currently an Associate Professor with Khalifa University, Abu Dhabi, United Arab Emirates. He is also a Visiting Reader at the Faculty of Engineering, University of Surrey, Surrey, U.K. His research interests include advanced digital signal processing techniques for communications, cooperative communications, vehicular communications, MIMO systems, and machine learning. He has authored over 150 journal and conference papers on these topics.

Dr. Muhaidat has been a Senior Editor for the IEEE COMMUNICATIONS LETTERS, and an Associate Editor for the IEEE TRANSACTIONS ON VEHICULAR TECHNOLOGY, while he currently serves as an Area Editor for the IEEE TRANSACTIONS ON COMMUNICATIONS. He was a recipient of several scholarships during his undergraduate and graduate studies. He was a winner of the 2006 NSERC Post-Doctoral Fellowship Competition.

Paul Yoo (M'11-SM'13) is currently with the CSIS within Birkbeck College at the University of London. Prior to this, he held academic/research posts in Cranfield (Defence Academy of the UK), Sydney (USyd) and South Korea (KAIST). He has amassed more than 60 prestigious journal and conference publications, has been awarded more than US 2.3 million in project funding, and a number of prestigious international and national awards for his work in advanced data analytics, machine learning and secure systems research, notably IEEE Outstanding Leadership Award, Capital Markets CRC Award, Emirates Foundation Research Award, and the ICT Fund Award. Most recently, he won the prestigious Samsung award for research to protect IoT devices.

Dr. Yoo serves as an Editor of IEEE COMML and Journal of Big Data Research (Elsevier). He is affiliated with the University of Sydney and Korea Advanced Institute of Science and Technology (KAIST) as a Visiting Professor. He is a Senior Member of the IEEE.

Jie Liang (S'99-M'04-SM'11) received the B.E. and M.E. degrees from Xi'an Jiaotong University, China, the M.E. degree from National University of Singapore (NUS), and the Ph.D. degree from the Johns Hopkins University, Baltimore, Maryland, USA, in 1992, 1995, 1998, and 2003, respectively. Since May 2004, he has been with the School of Engineering Science, Simon Fraser University, Canada, where he is currently a Professor. In 2012, he visited University of Erlangen-Nuremberg, Germany, as an Alexander von Humboldt Research Fellow. From 2003 to 2004, he worked at the Video Codec Group of Microsoft Digital Media Division. From 1997 to 1999, he was with Hewlett-Packard Singapore and the Center for Wireless Communications, NUS.

Dr. Liang's research interests include Image and Video Coding, Multimedia Communications, Sparse Signal Processing, Computer Vision, and Machine Learning. He has served as an Associate Editor for the IEEE Transactions on Image Processing, IEEE Transactions on Circuits and Systems for Video Technology (TCSVT), IEEE Signal Processing Letters, Signal Processing: Image Communication, and EURASIP Journal on Image and Video Processing. He received the 2014 IEEE TCSVT Best Associate Editor Award, 2014 SFU Dean of Graduate Studies Award for Excellence in Leadership, and 2015 Canada NSERC Discovery Accelerator Supplements (DAS) Award.

Anhong Wang is currently a professor in the School of Electronics Information Engineering, Taiyuan University of Science and Technology (TYUST), China. She received her PhD in Multimedia Image Processing from Beijing Jiaotong University in 2009. Her research interests include image video coding and transmission, compressed sensing and secret image sharing.